Animating a Tippe Top using Numerical Methods

Pranav Joneja
May 8, 2017

Ph-235 Computational Physics
The Cooper Union for the Advancement of Science and Art

Table of Contents

Introduction

This project is a study of the dynamics of a special kind of spinning top known as a *tippe top*. A tippe top has a particular mass distribution such that it initially spins on its spherical end, then while spinning, the tippe top inverts itself and continues spinning on its extended stem. See this YouTube video for an example: https://youtu.be/AyAgeUneFds

Figure 1: Physical Tippe Top

The dynamics of this peculiar spinning top has been a curiosity of physicists for decades. The origin of research on the topic can be traced back to an article in the *American Journal of Physics* titled "The Tippe Top (Topsy-Turvy Top)" by William Pliskin, who was a contemporary of Niels Bohr. However, the seminal paper on the topic was Richard Cohen's "The tippe top revisited", also in the *American Journal of Physics*. Cohen's 1977 paper was the first to formalize a theory that explained the inversion of the tippe top as an effect of non-conservative friction forces and he also laid out a method for deriving its equations of motions. Cohen's paper was so influential that since its publication, all research on the dynamics of the tippe top have followed that paradigm. In the same regard, this paper follows that structure, too. The current state of research involves proposals of new concepts/methods for modelling the friction between the tippe top and the surface on which it spins. This paper will provide an overview of one of these concepts and demonstrate its application to a simulation of the tippe top.

In a word, the aim of this project is to produce an animation of the tippe top using numerical methods. The Lagrangian method is applied to derive a system of equations of motion that describe the tippe top's dynamics. The numerical method of choice for solving this system of ordinary differential equations is an adaptive fourth-

order Runge-Kutta method. The solution is processed through a coordinate transform and finally animated using VPython objects.

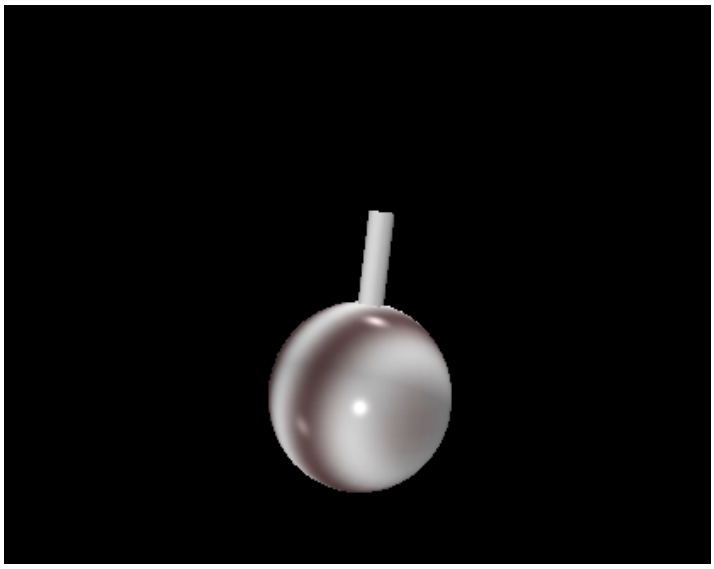

Figure 2: Mockup of a tippe top using a sphere object for the tippe top's main body and cylinder for the tippe top's stem. Both components are standard VPython objects.

Team Members, Roles, and Project Scope

As the sole contributor in this project, all research is conducted, code architected and algorithms implemented by me. Since this is an individual project, it is important that the scope of the project is kept small in order to keep it manageable. In this regard, some of the constraints on this project include:

- The components of the animation are kept minimal. The shape of the tippe top is approximated by only two standard VPython objects: sphere and a cylinder
- The UI of the program is bare bones. Implementing a neat UI for setting initial conditions and running simulations are 'bells-and-whistles' that are neglected in this project. This would be a very useful portion of future work though
- The model of the dynamics of the tippe top is limited to the duration starting at initial spin and ending when the stem touches the floor. While the model cuts off here, the real, physical tippe would continue to invert completely. For this portion, the model is significantly more mathematically and conceptually complex, and so is neglected for this project.

Approach

Before proceeding to study the dynamics of spinning objects, it is instructive to familiarize oneself with the Euler angles, a convenient coordinate system and reference frame for describing the motion of spinning objects. Figure 3 illustrates Euler angles in the context of a spinning top.

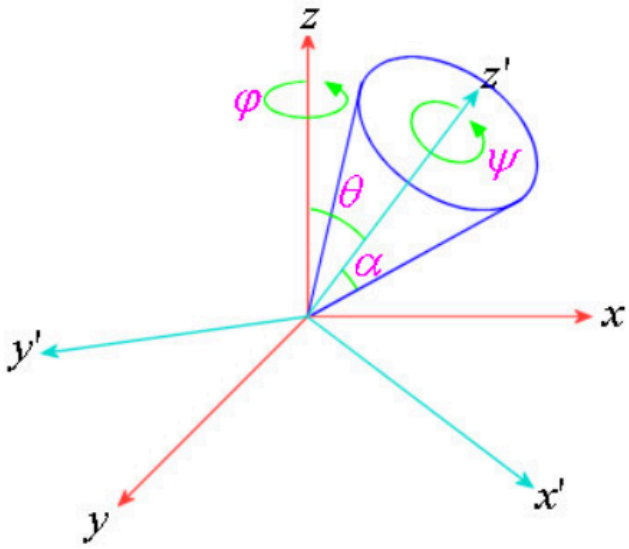

Figure 3: Euler angles in the context of a spinning top

There are two reference frames shown in Figure 3. The first (in red) is the reference frame of the lab. The z-coordinate always points vertically up in the lab, while the plane formed by the x- and y-coordinates is the horizontal plane on which the top spins. The second (in blue) is the 'body' reference frame of the spinning top. The z'-coordinate is aligned with the spinning top's primary symmetric axis.

The three Euler angles are nutation, precession and spin. Nutation (θ) is the angle between the vertical z-axis in lab frame and the body's primary symmetric z'-axis. Precession (ϕ *or* φ) is the angle around the vertical z-axis; in other words, precession lies in the lab's xy-plane. Finally, spin (ψ) is the angle around the body's z'-axis. It's important to note that a combination of these three Euler angles is sufficient to fully describe <u>any</u> possible orientation of the spinning object.

Armed with an understanding of Euler angles, it is now possible to begin deriving equations of motion for spinning objects. To become familiar with the general approaches of modelling spinning objects, a study of a ‘simple’ spinning top is considered first. The intention is to apply the Lagrangian method to derive the equations of motion for a simple spinning top before moving on to the study of more complex motion of a tippe top.

'Simple' spinning top dynamics

The structure of this section is as follows: (1) the equations of motion are derived using the Lagrangian method and presented in detail. (2) Next, the system of ODEs is solved using a simple (non-adaptive) fourth-order Runge Kutta method. (3) Finally, the solution is transformed from Euler angles to the animation or 'lab' frame.

Geometric definitions:

$m = mass\ of\ the\ top = 0.02\ kg$

$R = radius\ of\ the\ top = 0.02\ m$

l = length of the top along z'-axis = $0.04\ m$

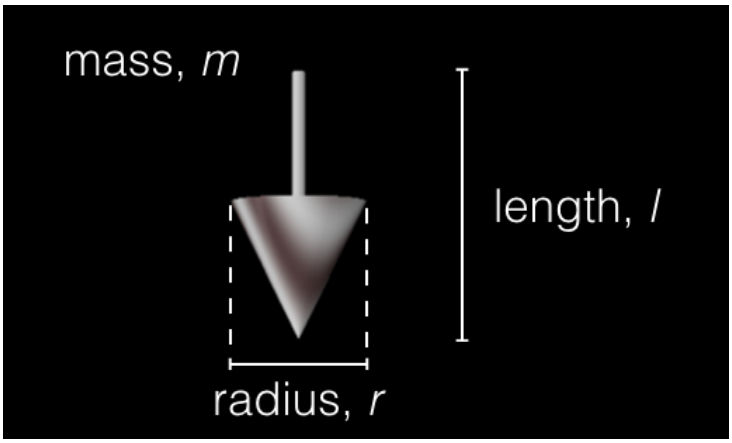

Figure 4: Geometry of the simple spinning top

Equations of Motion using Lagrangian Method

The textbook *Classical Dynamics* by Jorge V. José and Eugene J. Saletan provides an expression for Kinetic Energy of the spinning top system in terms of Euler angles.

$$T = \ Kinetic\ Energy = \frac{1}{2} I_1 \left(\dot{\theta}^2 + \dot{\phi}^2 sin^2(\theta)\right) + \frac{1}{2} I_3 \left(\dot{\psi} + \dot{\phi}\cos(\theta)\right)^2$$

where $I_1 = I_2 = \left(\frac{3}{20}\right) m \left(R^2 + \frac{l^2}{4}\right)$ (because the body is symmetric about x'- and y'- axes) meanwhile $I_3 = \left(\frac{3}{10}\right) mR^2$.

Secondly, an expression for Potential Energy is also derived

$$V = Potential\ Energy = mgl\cos\theta$$

Together, the Lagrangian is:

$$L = T - V = \frac{1}{2} I_1 \left(\dot{\theta}^2 + \dot{\phi}^2 sin^2(\theta)\right) + \frac{1}{2} I_3 \left(\dot{\psi} + \dot{\phi}\cos(\theta)\right)^2 - mgl\cos\theta \qquad \textbf{(1)}$$

The Lagrangian method for deriving equations of motion calls for taking derivatives of L with respect to each of the three Euler angles, as follows:

Nutation:

$$\frac{d}{dt}\left(\frac{dL}{d\dot{\theta}}\right) - \frac{dL}{d\theta} = 0$$

Taking derivatives appropriately:

$$\frac{dL}{d\theta} = \dot{\phi}^2 \sin(\theta)\cos(\theta)[I_1 - I_3] - I_3\dot{\phi}\dot{\psi}\sin(\theta) + mgl\sin(\theta)$$

$$\frac{d}{dt}\left(\frac{dL}{d\dot{\theta}}\right) = I_1\ddot{\theta}$$

So we have:

$$\frac{d}{dt}\left(\frac{dL}{d\dot{\theta}}\right) - \frac{dL}{d\theta} = I_1\ddot{\theta} - \dot{\phi}^2 \sin(\theta)\cos(\theta)[I_1 - I_3] + I_3\dot{\phi}\dot{\psi}\sin(\theta) - mgl\sin(\theta) = 0$$

$$\therefore \ddot{\theta} = \frac{\dot{\phi}^2 \sin(\theta)\cos(\theta)[I_1 - I_3] - I_3\dot{\phi}\dot{\psi}\sin(\theta) + mgl\sin(\theta)}{I_1} \qquad \textbf{(2)}$$

Precession:

$$\frac{d}{dt}\left(\frac{dL}{d\dot{\phi}}\right) - \frac{dL}{d\phi} = 0$$

$$\frac{dL}{d\phi} = 0$$

$$\frac{d}{dt}\left(\frac{dL}{d\dot{\phi}}\right) = I_1\ddot{\phi}\sin^2(\theta) + 2[I_1 - I_3]\dot{\phi}\dot{\theta}\sin(\theta)\cos(\theta) + I_3\ddot{\psi}\cos(\theta) - I_3\dot{\psi}\dot{\theta}\sin(\theta) + I_3\ddot{\phi}\cos^2(\theta)$$

And so:

$$\ddot{\phi} = \frac{2[I_3 - I_1]\dot{\phi}\dot{\theta}\sin(\theta)\cos(\theta) - I_3\ddot{\psi}\cos(\theta) + I_3\dot{\psi}\dot{\theta}\sin(\theta)}{I_1\sin^2(\theta) + I_3\cos^2(\theta)} \qquad \textbf{(3)}$$

Finally, spin:

$$\frac{d}{dt}\left(\frac{dL}{d\dot{\psi}}\right) - \frac{dL}{d\psi} = 0$$

$$\frac{dL}{d\psi} = 0$$

$$\frac{d}{dt}\left(\frac{dL}{d\dot{\psi}}\right) = I_3\ddot{\psi} + I_3\ddot{\phi}\cos(\theta) - I_3\dot{\phi}\dot{\theta}\sin(\theta)$$

Therefore:

$$\ddot{\psi} = \frac{I_3\dot{\phi}\dot{\theta}\sin(\theta) - I_3\ddot{\phi}\cos(\theta)}{I_3} = \dot{\phi}\dot{\theta}\sin(\theta) - \ddot{\phi}\cos(\theta) \qquad \textbf{(4)}$$

Now, equations **(3)** and **(4)** can be solved simultaneously resulting in the final form of the system of second-order ODEs:

$$\ddot{\theta} = \frac{\dot{\phi}^2\sin(\theta)\cos(\theta)[I_1 - I_3] - I_3\dot{\phi}\dot{\psi}\sin(\theta) + mgl\sin(\theta)}{I_1}$$

$$\ddot{\phi} = \frac{2[I_3 - I_1]\dot{\phi}\dot{\theta}\sin(\theta)\cos(\theta) - I_3\,\dot{\phi}\dot{\theta}\sin(\theta)\cos(\theta) + I_3\dot{\psi}\dot{\theta}\sin(\theta)}{I_1\sin^2(\theta)}$$

$$\ddot{\psi} = \dot{\phi}\dot{\theta}\sin(\theta) - \ddot{\phi}\cos(\theta)$$

***In this case, it will cause no problems to leave $\ddot{\psi}$ in terms of $\ddot{\phi}$ because $\ddot{\phi}$ can be computed before $\ddot{\psi}$ for each RK4 step*

Finally, to put the equations in a form that can be solved using RK4, we apply an important concept learned in the Ph-235 course: writing *N* second-order ODEs as *2N* first-order ODEs.

$$\begin{aligned} y_1 &= \dot{\theta} & \dot{y}_1 &= f(y_1, \theta, \phi, \psi) \\ y_2 &= \dot{\phi} & \dot{y}_2 &= f(y_2, \theta, \phi, \psi) \\ y_3 &= \dot{\psi} & \dot{y}_3 &= f(y_3, \theta, \phi, \psi) \end{aligned}$$

Transform from Euler angles to lab frame

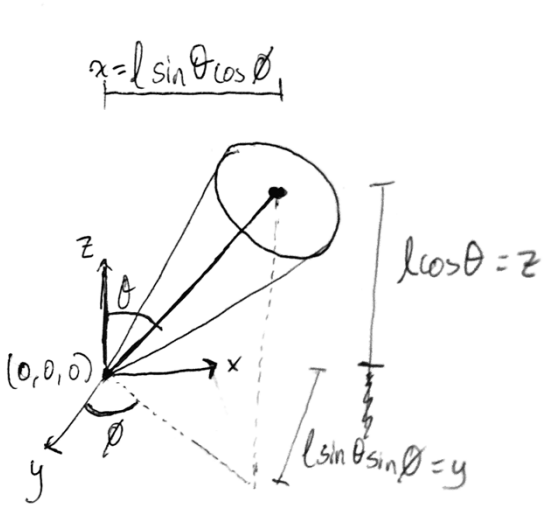

Figure 5 provides a visual argument in support of the following transformation from Euler angles (θ, ϕ, ψ) to lab frame (x,y,z).

In this example, the origin in the lab frame is fixed at (0,0,0). This is useful for the simple spinning top case because the model assumes friction can be neglected (because the contact point between the spinning top and the surface is infinitesimally small).

Figure 5: Coordinate transform (w/ origin fixed in lab frame)

The coordinate transform written as a matrix function is:

$$\begin{bmatrix} x \\ y \\ z \end{bmatrix} = \begin{bmatrix} l\sin(\theta)\cos(\phi) \\ l\sin(\theta)\sin(\phi) \\ l\cos(\theta) \end{bmatrix}$$

With these steps completed, the simple spinning top can be animated by implementing each of the steps above in Python. The attached script *simpletop_v.py* does exactly that.

Results of the Simple Spinning Top Animation

Plots of the nutation, rate of precession and spin rate each versus time can be obtained by running *simpletop.py* script.

With initial conditions:
$\theta_0 = 0.1\,rad, \phi_0 = 0.0\,rad, \psi_0 = 0.0\,rad$
$\dot{\theta}_0 = 0.0\,rad/s, \dot{\phi}_0 = 0.0\,rad/s, \dot{\psi}_0 = 155.0\,rad/s$

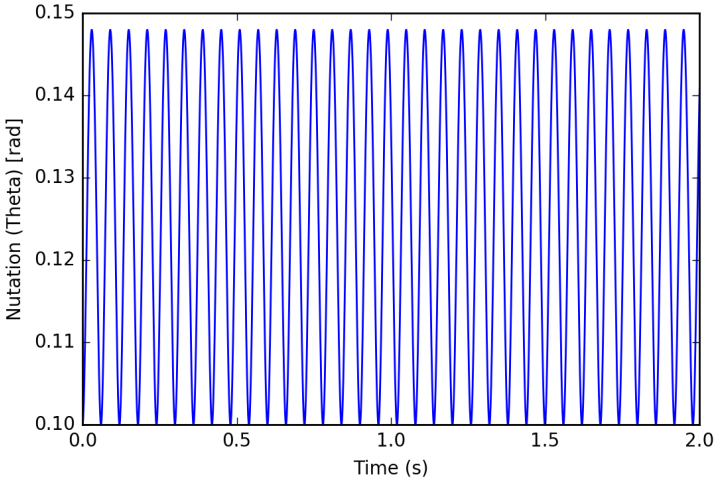

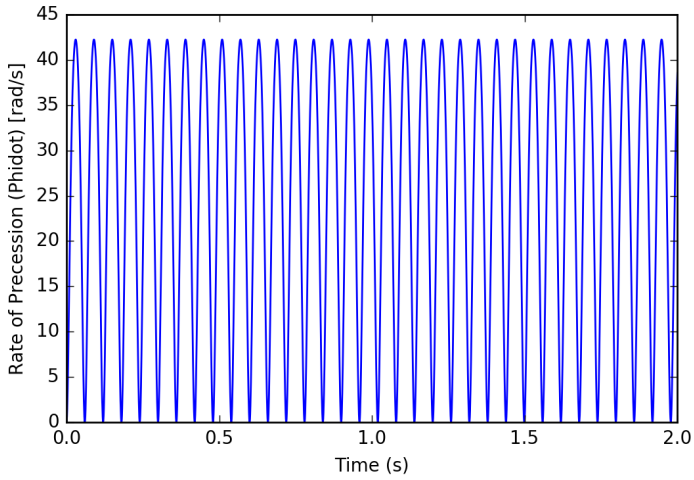

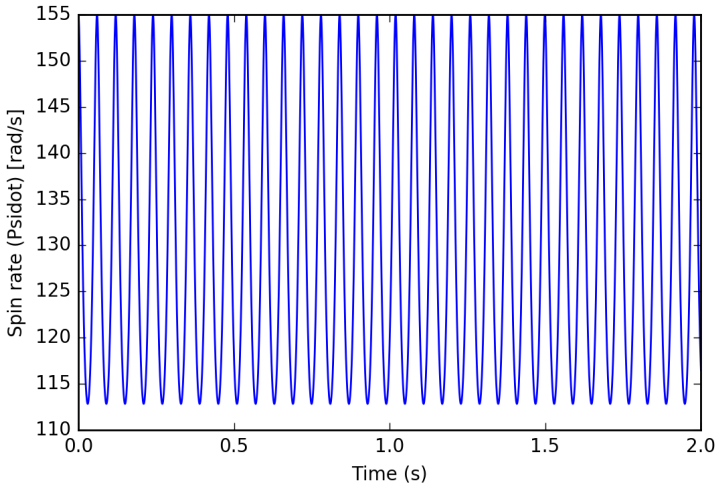

With initial conditions:
$\theta_0 = 0.1\, rad, \phi_0 = 0.0\, rad, \psi_0 = 0.0\, rad$
$\dot{\theta}_0 = 0.0\, rad/s, \dot{\phi}_0 = 0.0\, rad/s, \dot{\psi}_0 = 125.0\, rad/s$ (just slower initial spin rate)

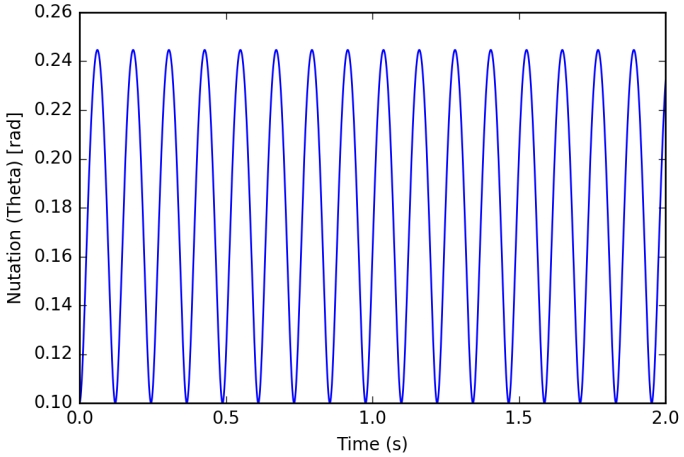

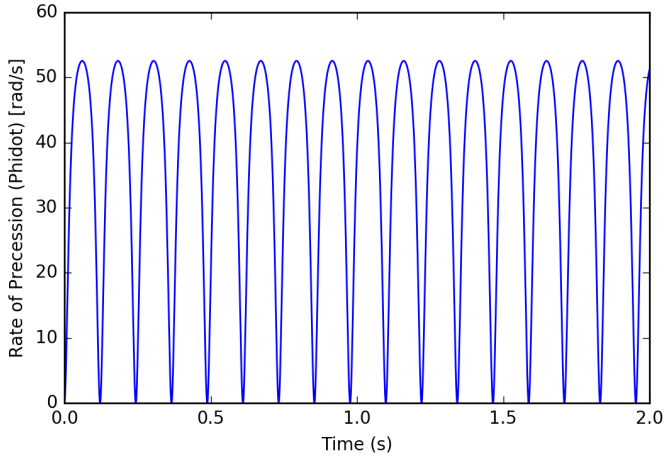

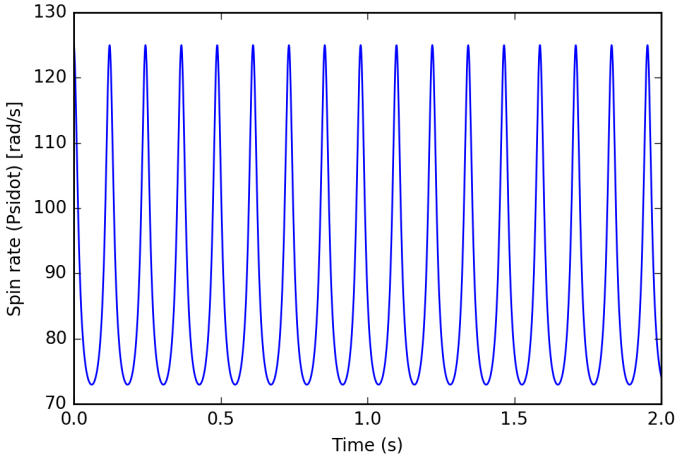

Correctness of RK4

To validate the results of this simulation, an in particular, prove that the RK4 method is implemented correctly, the following plot of Energy over time were generated.

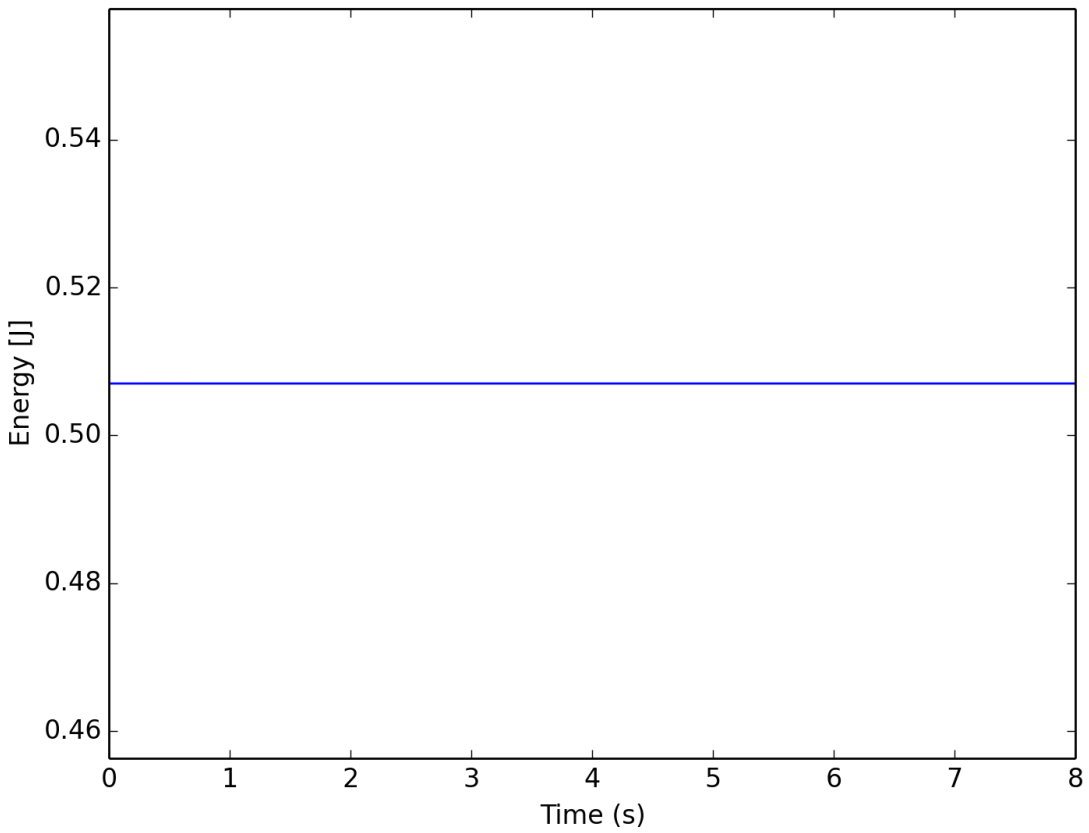

where the expression for energy in the system is:

$$E = T + V = \frac{1}{2} I_1 \left(\dot{\theta}^2 + \dot{\phi}^2 sin^2(\theta) \right) + \frac{1}{2} I_3 \left(\dot{\psi} + \dot{\phi} \cos(\theta) \right)^2 + mgl \cos\theta$$

Upon further inspection, the max. change in energy is: 2.458×10^{-6} J
In effect, this means energy is exceptionally well-conserved in the RK4 simulation, highlighting the accuracy and efficacy of its implementation.

Table 1 compares the results of the RK4 approximation at different step sizes. Since no 'exact' solution is available to compare to, the RK4 approximation for h = 0.00001 is used as an 'approximate exact' value. Since the RK4 method has fourth-order error, when the step-size is halved, the error should be smaller by a factor of 16. The error ratios in the last column of Table 1 are close to this theoretical error factor, which provides further confidence that the RK4 method in this simulation is correctly implemented.

Table 1: Comparison of RK4 step size to error of approximations

h	relative to h	Approximation to $\theta(1.0)$	Final Global Error $\theta(1.0) - "ym"$	Error Ratio
0.001	h	0.238970487651	-0.000361123124755	
0.0005	$\frac{1}{2}$ h	0.239300565741	-0.000031045034953	**12**
0.00025	$\frac{1}{4}$ h	0.239329564916	-0.000002045859334	**15**
0.000125	$\frac{1}{8}$ h	0.239331765409	-0.000000154312455	**13**
0.00001	<< h	"ym" = 0.239331610776		

Tippe Top dynamics

The approach to animating the tippe top follows very closely to the approach used to animate the simple top. The Lagrangian method is used once again to derive equations of motion, the RK4 method is used to solve

There are, however, a few key differences. These include:

- the model of the tippe top is vastly different to the model of the simple spinning top. This leads to different expressions for Kinetic and Potential energy in the Lagrangian Method.
- Friction is the force that plays the central role in causing the tippe top to invert. Since friction is a non-conservative force, energy is not conserved throughout the tippe top's inversion. In effect, the Lagrangian expression is not set equal to zero.
- An adaptive RK4 method is chosen instead of a fixed-step size one. This choice is conducive to more efficient computation.

Each of these key differences is explained in greater detail in the following sections.

Tippe Top model

$m = mass\ of\ the\ top = 0.02\ kg$

$R\ = radius\ of\ the\ top = 0.02\ m$

a = eccentricity of center of mass = 0.3

(distance of center of mass to geometric center as compared to radius of the top)

$I_1 = \left(\frac{131}{350}\right) mR^2$

$I_3 = \left(\frac{2}{5}\right) mR^2$

These parameters are based on a paper by Nils Rutstam [1].

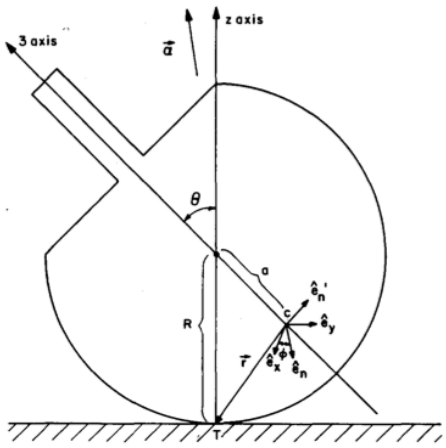

Figure 6: Tippe Top geometry

Friction Potential Function

Richard Cohen's paper provides an elegant argument that concludes that friction is the non-conservative force that causes the tippe top to invert. The fundamental elements of his argument are presented here in summary:

1. The tippe top is physically observed to invert. Since the center of mass started 'low' and ended 'higher', the potential energy of the system must have increased.
2. The spin rate of the tippe top is physically observed to slow down during its inversion. Since the top started with a 'fast' spin rate and ended with a 'slow' spin rate, the kinetic energy of the system must have decreased.
3. In the tippe top's own frame of references, its angular momentum is observed to reverse direction. This can be shown using a right hand rule, as depicted in Figure 7.
4. The 'usual suspects' for non-conservative forces are gravity and inertia, but these act on the body at its center of mass. Thus, neither gravity nor inertia can be responsible for this reversal of angular momentum.
5. The only remaining non-conservative force that could play a role is friction at the area of contact between the tippe top and the lab table surface.

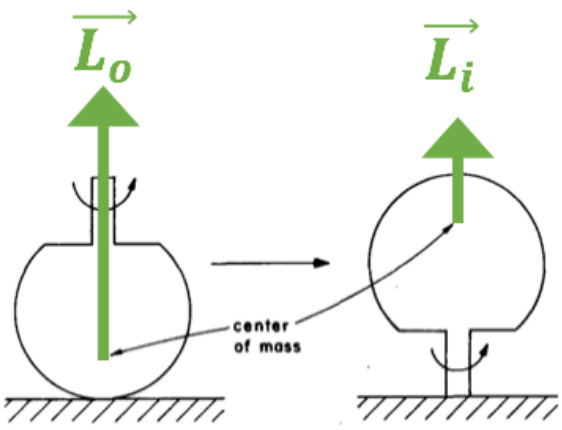

Figure 7: In the tippe top's own reference frame, angular momentum (L) is observed to reverse during inversion

Further investigation of the role of friction by other researchers revealed new concepts about friction. In particular, two researchers Leine and Glocker published a theory of the existence of a friction potential function. They theorize that such a potential function would depend on the tippe top's gliding (v) and spinning (ωR). Leine and Glocker produced RK4 simulations based on this model and included them in their paper. Furthermore, Rutstam, in his own paper, made simplifications to that model and found that his own model also this agrees with this result. All of this is to say, simply, that it is safe to use Rutstam's model as it agrees with the argument put forth by Richard Cohen and builds on the proven results of Leine and Glocker.

Equations of Motion

Using a non-conservative Lagrangian method, where Rutstam's friction potential function are included on the right hand side of the Lagrangian equation, leads to a derivation of the equations of motion of a tippe top. In lieu of the detailed derivation presented in Rutstam's full paper, the final vastly simplified equations of motion used in Rutstam's model are presented below:

$$\ddot{\theta} = \frac{\sin\theta}{I_1}\left(I_1\dot{\varphi}^2\cos\theta - I_3\omega_3\dot{\varphi} - R\alpha g_n\right) + \frac{R\mu g_n v_x}{I_1}(1-\alpha\cos\theta), \tag{10}$$

$$\ddot{\varphi} = \frac{I_3\dot{\theta}\omega_3 - 2I_1\dot{\theta}\dot{\varphi}\cos\theta - \mu g_n v_y R(\alpha-\cos\theta)}{I_1\sin\theta}, \tag{11}$$

$$\dot{\omega}_3 = -\frac{\mu g_n v_y R\sin\theta}{I_3}, \tag{12}$$

$$\dot{v}_x = \frac{R\sin\theta}{I_1}\left(\dot{\varphi}\omega_3\left(I_3(1-\alpha\cos\theta)-I_1\right) + g_n R\alpha(1-\alpha\cos\theta) - I_1\alpha(\dot{\theta}^2+\dot{\varphi}^2\sin^2\theta)\right) - \frac{\mu g_n v_x}{mI_1}\left(I_1 + mR^2(1-\alpha\cos\theta)^2\right) + \dot{\varphi}v_y, \tag{13}$$

$$\dot{v}_y = -\frac{\mu g_n v_y}{mI_1 I_3}\left(I_1 I_3 + mR^2 I_3(\alpha-\cos\theta)^2 + mR^2 I_1\sin^2\theta\right) + \frac{\omega_3\dot{\theta}R}{I_1}\left(I_3(\alpha-\cos\theta) + I_1\cos\theta\right) - \dot{\varphi}v_x, \tag{14}$$

$$g_n = \frac{mgI_1 + mR\alpha\left(\cos\theta\left(I_1\dot{\varphi}^2\sin^2\theta + I_1\dot{\theta}^2\right) - I_3\dot{\varphi}\omega_3\sin^2\theta\right)}{I_1 + mR^2\alpha^2\sin^2\theta - mR^2\alpha\sin\theta(1-\alpha\cos\theta)\mu v_x}.$$

where $\theta, \varphi, \omega_3$ are equivalent to θ, ϕ, ψ (he same Euler angles previously described). And v_x and v_y are components of velocity of the center of mass of the tippe top.

As such, the tippe top's motion is completely described by the six variables:
$\theta, \dot{\theta}, \dot{\varphi}, \omega_3, v_x, v_y$

$\mu = 0.3$, an assumed coefficient of friction
And g_n is an "effective gravity" factor that plays a role in determining the magnitude of friction

Energy is not conserved

It is worthwhile reiterating that energy is not conserved in the tippe top system. As such, there is no point in attempting to determine the correctness of the RK4 method implemented here by plotting energy over time. In addition, since an adaptive RK4 method is implemented, the ability to check correctness by 'halving' the RK4 stepsize and comparing the error in approximations is also taken away.
Still, there is confidence that the RK4 method here is implemented correctly because the bare structure of the code is based on the spinning top code presented earlier in this paper. In addition, inspection of the results here show that they closely match the results of previous papers by Cohen, Rutstam and others.

Results of the Tippe Top Animation

Plots of the nutation, rate of precession and spin rate each versus time can be obtained by running *tippe_adaptive.py* script.

The full animation of tippe top is presented by running *tippe_adaptive_v.py*

With initial conditions:

$\theta_0 = 0.1\,rad, \dot{\theta}_0 = 0.1\,rad/s, \dot{\phi}_0 = 0.0\,rad/s, \omega_{3_0} = 155.0\,rad/s$

$v_{x_0} = 0.0\frac{m}{s}, v_{y_0} = 0.0\frac{m}{s}$

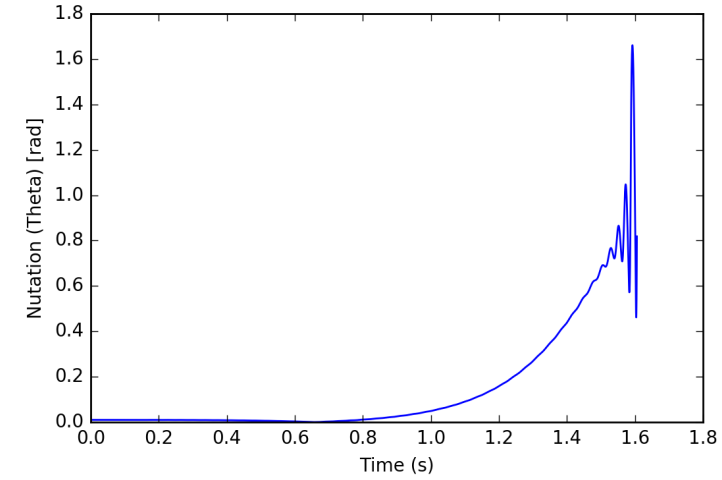

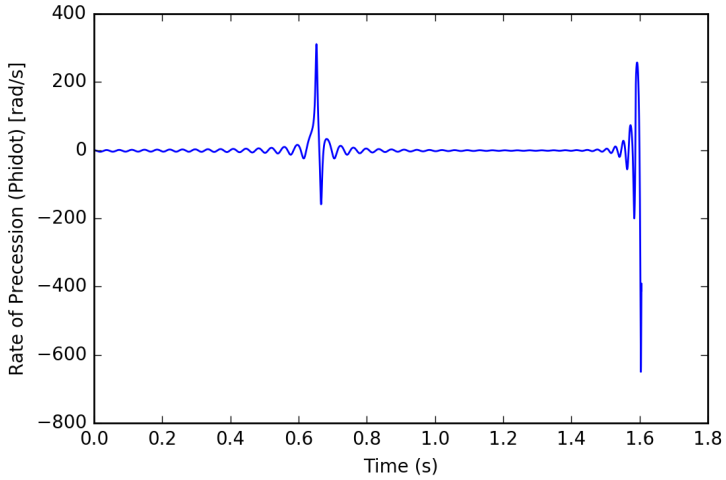

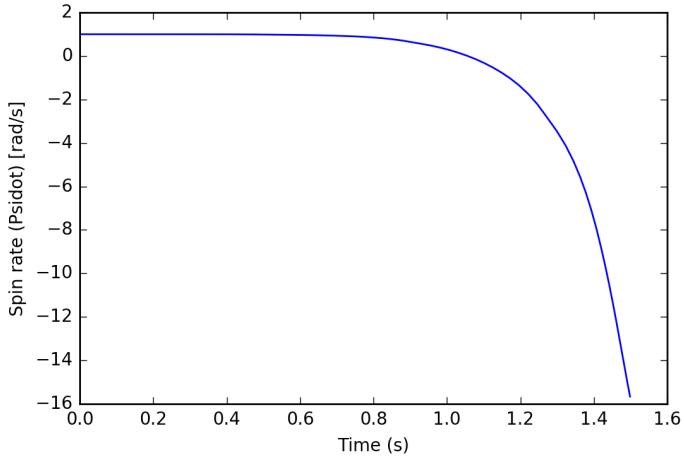

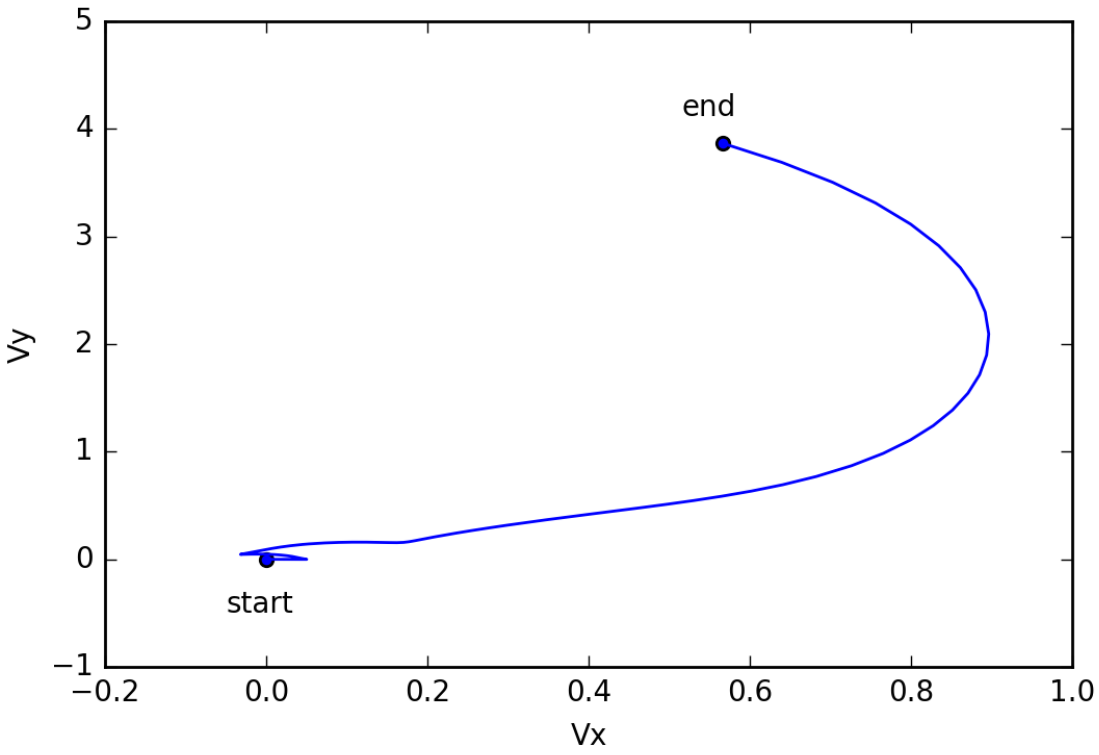
end
start
Vy
Vx
5
4
3
2
1
0
−1
−0.2
0.0
0.2
0.4
0.6
0.8
1.0

With initial conditions:

$\theta_0 = 0.1\,rad, \dot{\theta}_0 = 0.1\,rad/s, \dot{\phi}_0 = 0.0\,rad/s, \omega_{3_0} = 755.0\,rad/s$

$v_{x_0} = 0.0\frac{m}{s}, v_{y_0} = 0.0\frac{m}{s}$

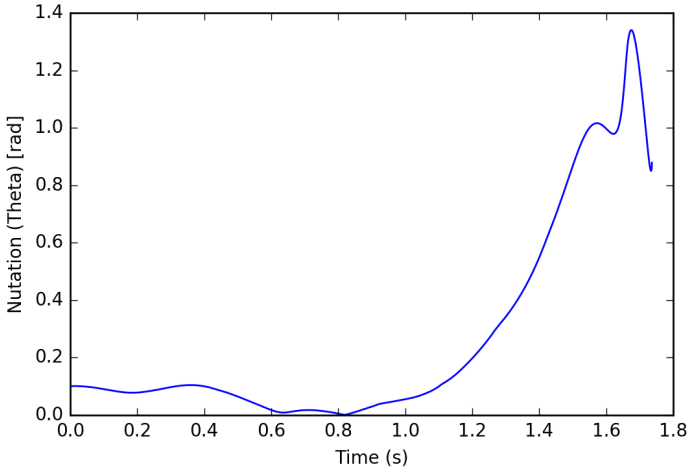

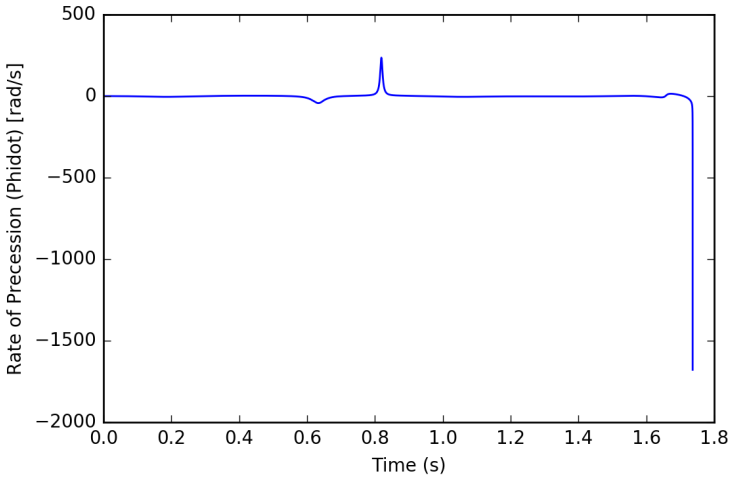

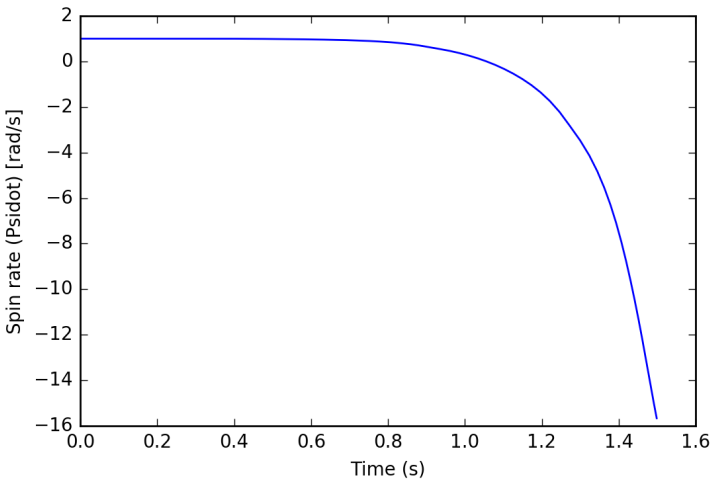

References

Tippe Top Equations and Equations for Related Mechanical Systems by Nils Rutstam. [http://www.emis.ams.org/journals/SIGMA/2012/019/sigma12-019.pdf]

José, Jorge Valenzuela, and Eugene Jerome Saletan. *Classical Dynamics: A Contemporary Approach*. Cambridge: Cambridge UP, 2013. Print.

Cohen, Richard J. "The Tippe Top Revisited." *American Journal of Physics* 45.12 (1977): 12-17.

Friedl, Christian. "Der Stehaufkreisel." Universität Augsburg, Institut für Physik. 1997

Leine, Remco I., and Christoph Glocker. "A Set-Valued Force Law for Spatial Coulomb-Contensou Friction." *Volume 5: 19th Biennial Conference on Mechanical Vibration and Noise, Parts A, B, and C* (2003): n. pag. Web.

Numerical Simulation, Animation by Christian Friedl and André Wobst. [http://www.wobsta.de/uni/tippetop/movie.shtml.en]

Motion of the Tippe Top: Gyroscopic Balance Condition and Stability by Takahiro Ueda, Ken Sasaki, and Shinsuke Watanabe. [https://arxiv.org/abs/physics/0507198v1]